MRJF4, a novel histone deacetylase inhibitor, induces *p21* mediated autophagy in PC3 prostate cancer cells

V. Di Giacomo[1], V. Di Valerio[2], M. Rapino[3], D. Bosco[3], I. Cacciatore[1✉], M. Ciulla[1], A. Marrazzo[4], J. Fiorito[5], A. Di Stefano[1] and A. Cataldi[1]

[1] Department of Pharmacy, University G. d'Annunzio, Via dei Vestini 31, 66100 Chieti, Italy

[2] Department of Medicine and Aging Sciences, Via dei Vestini 31, 66100 Chieti, Italy

[3] Institute of Molecular Genetics of CNR, Via dei Vestini 6, 66100 Chieti, Italy

[4] Department of Pharmaceutical Sciences, University of Catania, V.le A. Doria 6, 95125 Catania, Italy

[5] Department of Pathology and Cell Biology and Taub Institute for Research on Alzheimer's Disease and the Aging Brain, Columbia University, 630 W 168th St., New York, NY 10032, USA

Corresponding author: : I. Cacciatore, Department of Pharmacy, University G. d'Annunzio, Via dei Vestini 31, 66100 Chieti, Italy. E-mail: cacciatore@unich.it

Abstract

Autophagy is a cellular defense mechanism which occurs through degradation and recycling of cytoplasmic constituents and represents a caspase-independent alternative to cell death by apoptosis. It is generally accepted that the suppression of autophagy in many cancer cells is directly correlated to malignancy; hence, the control of autophagy genes could represent a target for cancer therapy. The inhibition of cell proliferation through autophagy activation could be an important mechanism for many anti-tumor drugs. Here we report the effects of a novel histone deacetylase inhibitor MRJF4 (racemic mixture) and of its two enantiomers [(+)-MRJF4 and (-)-MRJF4] on the morphological and molecular mechanisms causing death and migration of PC3 prostatic cancer cells. In particular, we investigated the occurrence of the autophagic process, both at morphological and molecular levels (LC3 expression), and its relationship with *p21*, a key molecule which regulates cell cycle and autophagy cell death. Moreover, pERK/Nf-kB driven intracellular signaling, the expression of MMP9 protein - a key component of cell migration - invasion, and metastasis were assayed. Our results showed that the anti-proliferative effects of MRJF4 due to autophagy occurrence, documented by LC3 increase and ultrastructural modifications, and the reduction of invasiveness seem to be mediated by the down-regulation of pERK/NF-kB signaling pathway, along with *p21* up-regulation.

Key words: Autophagy, Histone deacetylase inhibitor, MRJF4, PC3 prostate cancer cells, *p21*, pERK/NF-kB.

Introduction

Autophagy is a cellular defense mechanism which occurs through degradation and recycling of cytoplasmic constituents; it represents a caspase-independent alternative to cell death by apoptosis but, as well as the latter one, implies mitochondrial involvement (1). Authophagy is a fundamental and phylogenetically conserved self-degradation process characterized by two steps: a) formation of autophagosomes containing morphologically intact cytosol or organelles; b) formation of degradative autophagic structures (autolysosomes) containing partially degraded cytoplasmic and organelles (2). During the formation of mammalian autophagosomes, LC3 target protein modification is essential to the process and represents an autophagosomes marker (3). Moreover, it has been generally accepted that autophagy is suppressed in many cancer cells and that cellular autophagic activity is inversely correlated to malignancy (4). Thus, the breakdown of the autophagy process may contribute to the development of cancer and, conversely, control/execute autophagy genes could represent a target for cancer therapy; in fact, the inhibition of cell proliferation through autophagy activation could be an important mechanism for many anti-tumor drugs. Data report that the treatment of breast carcinoma cell line MCF-7 with the estrogen antagonist tamoxifen (5), as well as the treatment of malignant glioma cells with arsenic trioxide (6), caused authopagy-mediated cell death. Furthermore, autophagy is tightly linked to endoplasmic reticulum stress (ERS) response which can be triggered by disparate mechanisms including histone deacetylase (HDAC) inhibition. Histone deacetylase inhibitors (HDACi) constitute a structurally diverse group of pharmacological agents, primarily known for their epigenetic control of gene transcription (7-9), cell growth arrest, and apoptosis occurrence in cancer (10). In particular, recent reports have established a link between HDACi and ERS (11). Lately, the novel multi-target ligand MRJF4 (sigma-1 antagonist, sigma-2 agonist, and HDACi) has been prepared and suggested as a new potential tool for the treatment of prostate and brain cancers (12-14).

Here, to further explore the pharmacological profile of this new multi-target ligand, we have studied the effect of MRJF4 (racemic mixture) and its two enantiomers [(+)-MRJF4 and (-)-MRJF4] on the morphological and molecular mechanisms driving PC3 prostatic cancer cells to death and migration. In particular, we have investigated the occurrence of the autophagic process both at morphological and molecular levels (LC3 expression) and its relationship with: a) *p21*, a key molecule which regulates cell cycle and autophagy cell death (15, 16); b) pERK/Nf-kB driven intracellular signaling (17); c) the expression of metalloproteinase-9 (MMP9), a key component of cell migration and invasion mecha-

nisms (18-20).

Materials and methods

Cell culture and treatment

PC3 human prostate cancer cells were purchased from the American Type Culture Collection (ATCC) and maintained in RPMI 1640 supplemented with 2 mM Glutamine, 100 μg/mL penicillin-streptomycin, and 10% FBS. Cells were grown at 37 °C in a humidified atmosphere of 5% CO_2 and treated from 6 to 72 hours with 5 μM (±)-MRJF4, (+)-MRJF4, and (-)-MRJF4, synthesized as previously reported (12), and with commercial 4-phenylbutyric acid (PhBA) and haloperidol metabolite II [(±)-HP-mII]. The chosen concentration was 5 μM based on previously published data on C6 rat glioma cells using the prodrug (obtained through conjugation of (±)-HP-mII to PhBA via an ester bond) concentrations ranging from 0.1 to 5 μM, as elsewhere reported (14). Regarding time points, longer time intervals (24-72 h) were chosen to evaluate changes in biological parameters like cell viability and apoptosis occurrence, while shorter treatments (6-24 h) were used to investigate the effects on protein expression and modifications (i. e. phosphorylation and acetylation).

Cell viability assay

Cell viability was measured by MTT (3 [4,5-dimethylthiazol-2yl]-2,5-diphenyl tetrazolium bromide) growth assay (Sigma Aldrich, St Louis, USA). Cell number was quantified by the amount of tetrazolium reduction in viable mitochondria (21). Cultured cells were seeded into 24-well plate at 5×10^4 cells/well and exposed to 5 μM concentration of each compound. After 24 and 48 h cells were processed according to manufacturer's instructions and the absorbance of each sample was detected at 570 nm. Percentage of viable cells was calculated using the equation $A_s/A_0 \times 100$ where A_s is the absorbance value obtained for a sample containing cells in the presence of a given concentration of agent, and A_0 is the absorbance value of vehicle treated control. Four independent experiments were performed under the same experimental conditions.

Flow cytometry detection of acetylated histone H4

PC3 cells were stained for hyperacetylated histone 4 (penta-H4) as previously described (22). Briefly, after incubation, cell culture medium was removed and cells fixed for 15 min in 1% *p*-formaldehyde on ice. Then, cells were trypsinized and pellets were washed with 1% PBS/BSA and centrifuged at 130 g for 10 min at 4 °C. Cells were permeabilized in 0.1% Triton X-100/PBS for 10 min and pellets were resuspended in 10% goat serum/PBS and incubated for 20 min on ice. Anti-hyperacetyl histone-H4 rabbit polyclonal antibody (Merck Millipore, NH, USA) was added to the solution (1:100) and incubated for 1 h on ice. Primary antibody was removed and a FITC-conjugated goat anti-rabbit IgG (H+L) secondary antibody (Millipore) was added and incubated on ice in the dark for 45 min. Secondary antibody was removed and, prior to running on the FC500, cells were resuspended in PBS/BSA. About 10000 events were collected for all samples using 488 nm laser excitation and analyzed with CXP software (Beckmann Coulter,

FL, USA). Mean fluorescence intensity (MFI) was obtained by histogram statistics.

Annexin-V/PI detection of apoptotic and necrotic cells in flow cytometry

To assess apoptosis a commercial Annexin V-FITC/PI Kit (Bender Med System, Vienna, Austria) was used according to the manufacturer's instructions. Briefly, 2.5×10^5 cells were gently suspended in binding buffer and incubated for 10 min at room temperature in the dark with Annexin-V-FITC (23). Samples were then washed, supravitally stained with propidium iodide (PI), and analyzed on a FC500 flow cytometer with the FL1 and FL3 detector in a log mode using the CXP analysis software (Beckman Coulter). For each sample, at least 10^4 events were collected. Viable cells were Annexin-V^{neg}/PI^{neg} (unlabelled), early and late apoptotic cells were Annexin-V^{pos}, and necrotic cells were Annexin-V^{neg}/P^{pos} (24).

Immunofluorescence microscopy analysis

Cells grown in slide chambers were fixed in 4% paraformaldehyde for 10 min and washed in PBS, then permealized in 0.1% Triton X-100, incubated in 5% goat serum in PBS at room temperature and in the presence of 10 μg anti-LC3B rabbit polyclonal antibody (Sigma, San Louis, MI, USA) in PBS, 5% Tween -20, 2% BSA for 1 h at 37 °C. After two washings in PBS, slides were allowed to react with FITC-conjugated goat anti-rabbit immunoglobulin antibody in PBS, 5% Tween-20, 2% BSA. Nuclei were counterstained with glycerol DABCO (1-4-diazabicyclol [2-2-2]octane) containing 5 μg/mL DAPI (4-6 diamidino-2-phenyl-indol) (Santa Cruz, Santa Cruz Biotechnology, CA, USA) for 5 min at room temperature. The negative control, performed by omitting the primary antibody, has not been subjected to FITC staining (25). The labelled slides were observed with a Leica DM4000 fluorescence microscope equipped with Leica DFC 320 videocamera (Leica Cambridge Ltd, Cambridge, UK) to acquire computerized images.

Computerized morphometry measurements and image analysis

After digitizing the images deriving from immunofluorescence, Leica Qwin 3.5 Plus Software System (Leica Cambridge Ltd) was used to evaluate LC3 expression. Image analysis of protein expression was performed through the quantification of thresholded areas for immunocytochemical fluorescent colour per ten fields of light microscope observation. LeicaQwin-Plus 3.5 assessments were logged to Microsoft Excel and processed for Percentage, Standard deviations, and Histograms.

Transmission electron microscopy

Pelleted cells were fixed in 1% glutaraldehyde in 0.1 mol/L phosphate buffer pH 7.6 for 1 h at 4 °C. After two washings in phosphate buffer, samples were post fixed in 1% osmium in 0.1 M phosphate buffer for 1 h, acetone dehydrated, embedded in Epon 812 catalyzed for 3 days at 60 °C. Semithin sections (700 nm) were Toluidine blue stained (1% in H_2O) and observed in light microscopy. Ultrathin sections (80 nm) were counterstained using uranyl acetate and lead citrate, mounted
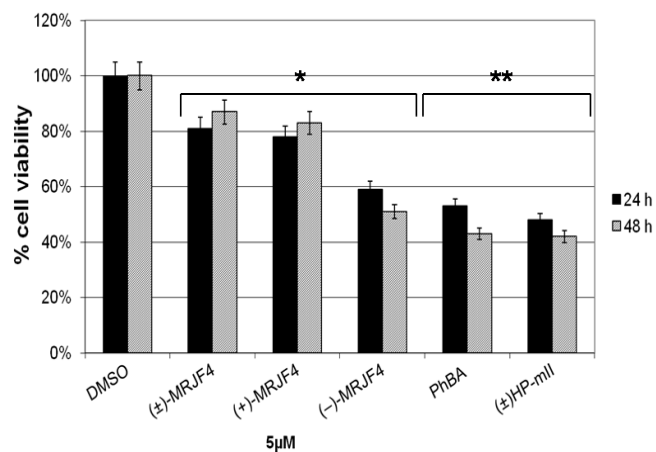
Figure 1. Effect of 5 µM (±)-MRJF, (+)-MRJF, (-)-MRJF, PhBA and (±)-HP-mII compounds on PC3 prostate cancer cells proliferation (n=4). Graphs show results of MTT assay after 24 and 48 h of treatment. *p < 0.05 and **p < 0.01 relative to control sample.
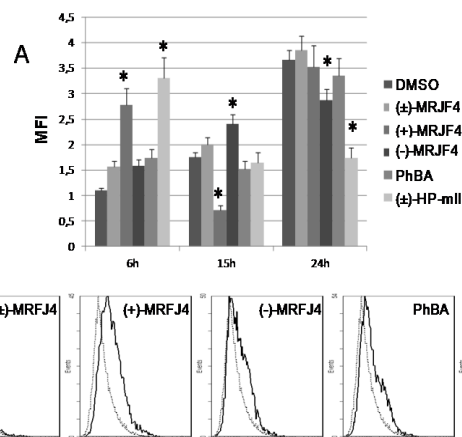

Figure 2. Effect of 5 µM (±)-MRJF, (+)-MRJF, (-)-MRJF, PhBA and (±)-HP-mII compounds on histone H4 acetylation in PC3 cells (n=3). **A**: Graph shows the mean MFI (Mean Fluorescence Intensity) ± SD of hyperacetylated H4 after 6, 15 and 24 h of treatment. *p < 0.05 relative to control sample. **B**: Histograms are representative of 6 h treatment. In each histogram the indicated sample (continuous line) is plotted with DMSO (dotted line).

on 300 mesh nickel grids, and processed for electron microscopy analysis.

Western blotting analysis

Total cell lysates (60 µg) were electrophoresed on a 10% sodium dodecyl sulphate (SDS)-polyacrylamide gel and transferred to nitrocellulose membrane. Nitrocellulose membranes, blocked in 5% BSA, 10 mmol/L Tris-HCl pH 7.5, 100 mmol/L NaCl, 0.1% Tween-20, were probed with mouse β-tubulin monoclonal antibody (Sigma, USA), mouse p-IkBα, IkBα, *p21* monoclonal antibodies (Santa Cruz, Santa Cruz Biotechnology, CA, USA), mouse anti-MMP9 monoclonal antibody (Calbiochem, Darmstadt, Germany), rabbit Erk polyclonal and rabbit p-Erk monoclonal antibodies (Cell Signalling, UK), incubated in the presence of specific enzyme-conjugated IgG horseradish peroxidase. Immunoreactive bands were detected by ECL detection system (Amersham Intl., Buckinghamshire, UK) and analysed by densitometry. Densitometric values, expressed as Integrated Optical Intensity (I.O.I.), were estimated by a CHEMIDOC XRS system by the QuantiOne 1-D analysis software (BIORAD, Richmond, CA, USA). Values were normalized basing on densitometric values of internal β-tubulin.

Migration assay

Cell migration was assayed by using a trans-well chamber containing a polycarbonate insert with 8 µm pores placed between the upper and lower well (Corning, NY, USA). Cells were cultured to 70-80% of confluence and starved for 24 h in serum free condition. PC3 cancer prostatic cells were then trypsinized, centrifuged, and resuspended in serum free HAM'S F12 at a concentration of 10^5 cells/mL. 100 µL of such suspension have been added to the upper chamber of the trans-well and 600 µL of HAM'S F12 with 5% FCS were added to the lower chamber. MRJF4 and its enantiomers, at a final concentration of 5 µM, were added 2 h later to allow cells to adhere to the membrane. After 24 h of incubation at 37 °C, cells on the upper side of the filter were removed with a cotton swab, while cells that migrated through the pores to the lower side of the membrane have been fixed with absolute methanol and stained with DAPI. Subsequently, the filter was cut out

with a scalpel, mounted on a slide, and nuclei counted under a microscope in five random fields of a known area.

To calculate migration, the total number of cells was determined counting and averaging the total number of cells in each of the random fields. The resulted number was divided by the area of the microscope viewing field and multiplied by the entire area of the trans-well insert. The result represented the total number of cells. Percentage of migration was calculated by dividing the total number of cells by the number of cells seeded and multiplying this value by 100.

Statistical analysis

The significance of the differences recorded between the diverse experimental conditions tested was evaluated using Student *t* test. Probability levels of < 0.05 were considered statistically significant.

Results

A reduction of viability of about 20% is observed in samples treated with either the racemic mixture or (+)-MRJF4. The (-)-MRJF4 enantiomer shows a reduction of viable cells below 50% after 24 and 48 h of treatment, comparable to the effects of PhBA and (±)-HP-mII (Figure 1). In parallel, to evaluate the inhibitory activity of our compounds on histone 4 (H4) deacetylase enzyme, flow cytometric acetylation assay was performed (Figure 2). After 6 h, H4 acetylation results mainly increased by (+)-MRJF4, similar to the effect exerted by (±)-HP-mII, while other compounds do not seem to affect histone acetylation. Anyway, after 15 h, (+)-MRJF4 seems to significantly reduce H4 acetylation, while (-)-MRJF4 shows a slight inhibitory effect on HDAC. After 24 h, all the compounds show an effect on histone acetylation similar to or lower than the control sample. To understand if apoptosis occurrence justifies the observed viability reduction, an Annexin-V/PI assay was performed at 24, 48, and 72 h time intervals and no difference was evidenced upon treatment in all the experimental conditions (Figure 3).
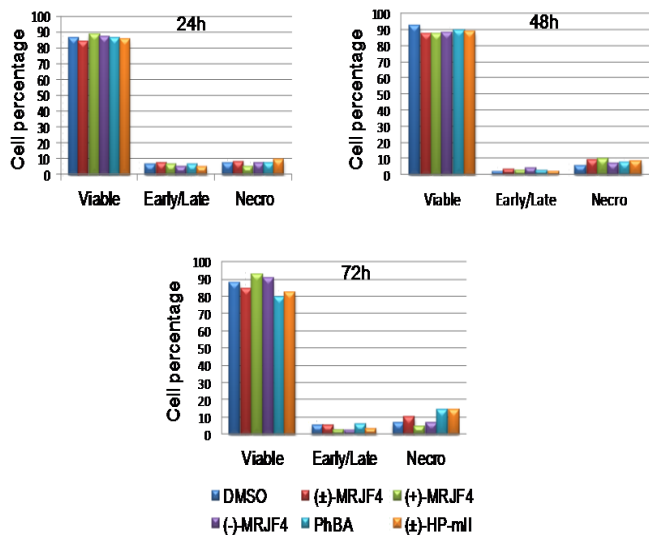
Figure 3. Annexin/PI detection of apoptotic and necrotic cells in PC3 cells treated with 5 μM (±)-MRJF4, (+)-MRJF4, (-)-MRJF4, PhBA and (±)-HP-mII compounds for 24, 48 and 72 h (n= 3).
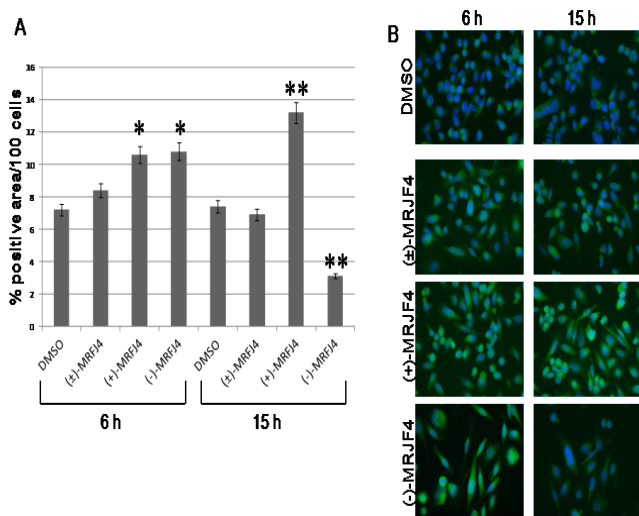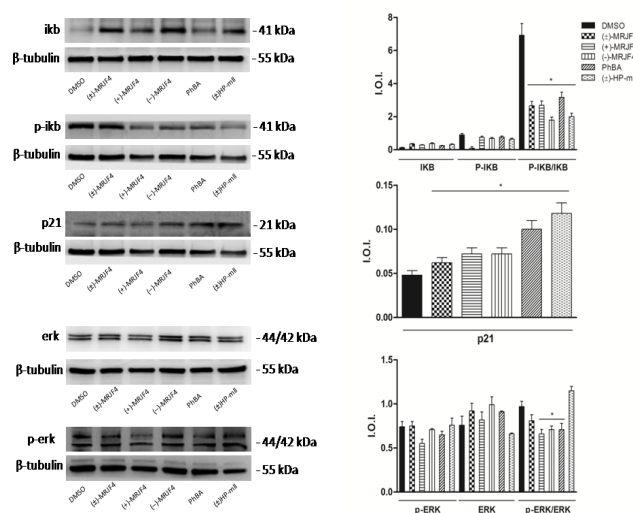

Figure 4. Effect of 5 μM (±)-MRJF4, (+)-MRJF4, (-)-MRJF4, PhBA and (±)-HP-mII compounds on LC3 expression in PC3 cells after 6 and 15 h of treatment (n=3). A) Histogram shows the mean percentage (± SD) of positive area/100 cells B) Representative images of PC3 cells staining with LC3 antibody. *p < 0.05 and **p < 0.01 relative to control sample.

Thus, autophagy occurrence has been hypothesized in response to HDACi treatment. In fact, while after 6 h of treatment both (+)- and (-)-MRJF4 show a significant increase in the expression of the autophagy marker LC3, after 15 h it is mainly increased upon (+)-MRJF4 treatment (Figure 4). This evidence was supported by electron microscopy analysis, performed after 24 h of treatment, which disclosed autophagic features like a large amount of free membrane structures and double membranes into the cytoplasm. Free membrane structures seemed to be pre-autophagosomes which turned into autophagosomes containing portions of organelles, such as endoplasmic reticulum and mitochondria. Control cells did not disclose any of these modifications (Figure 5). The phosphorylation rate of Erk seems to be downregulated by the racemic mixture as well as by the two enantiomers. A similar behaviour is observed for the IkB-α phosphorylation, while *p21* expression shows an increase at all the experimental points (Figure 6). In addition, the invasiveness of such cells was investigated by trans-well migration test showing that, upon (±)-
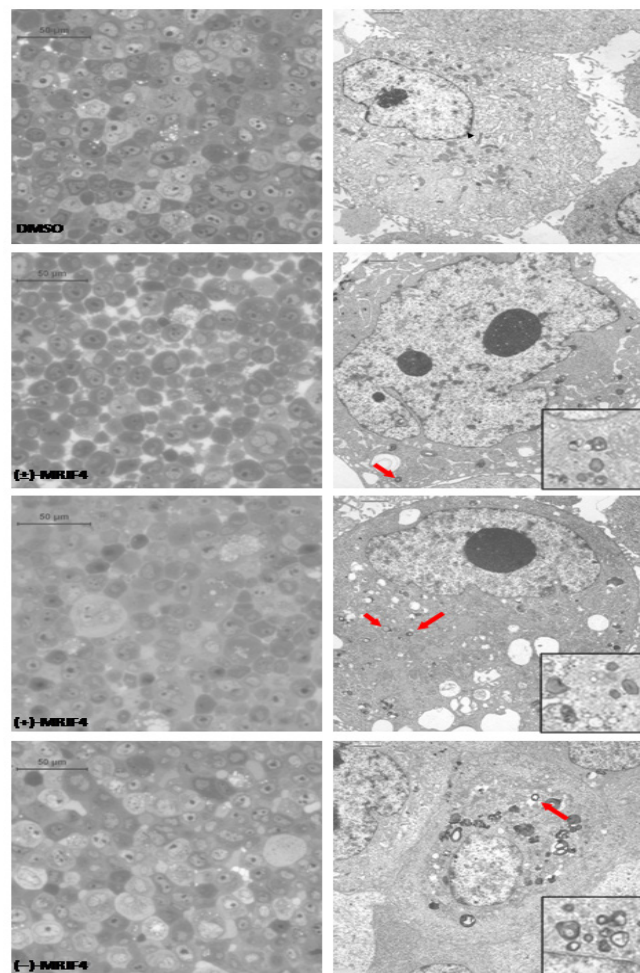

Figure 5. Toluidine blue stained semithin sections (left panel, magnification: 40x) and electron microscopy pictures (right panel, magnification: 3000x) of PC3 prostatic cancer cells treated with 5 μM (±)-MRJF4, (+)-MRJF4 and (-)-MRJF4 for 24 h. Arrows indicate the autophagic structures showed at higher magnification (30000x) in the inserts.

Figure 6. A: Effect of 5 μM (±)-MRJF4, (+)-MRJF4, (-)-MRJF4, PhBA and (±)-HP-mII compounds on Erk, ikBα and *p21* protein expression and/or phosphorylation in PC3 cells after 6 h of treatment (n=3). **A** Each blot is the most representative. **B**: Densitometric analysis (mean ± SD). *p < 0.05 relative to control sample.

MRJF4, (-)-MRJF4, and (+)-MRJF4 treatment, cells migration capability was reduced to 70% for the first, 66% for the second, and 52% for the third one (Figure 7 A and B). The expression of MMP9 protein, a key enzymatic component of cell migration and invasion, is
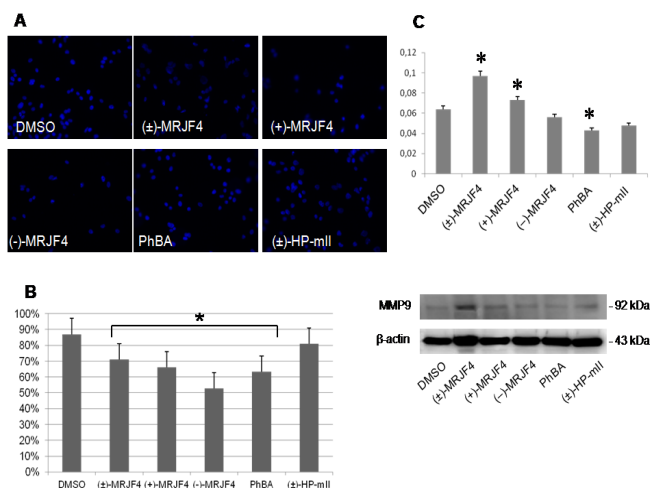
Figure 7. Effect of 5 μM (±)-MRJF4, (+)-MRJF4, (-)-MRJF4, PhBA and (±)-HP-mII compounds on PC3 prostate cancer cells migration after 24 h of treatment (n=3). **A**: Representative images of PC3 cells staining with DAPI. **B**: Histogram shows the mean percentage (± SD) of PC3 cells attached to the membrane downsides of trans-well migration chamber. **C**: Western blotting analysis of MMP9 protein expression performed after 6 h of treatment (n= 3). The most representative blot and the densitometric analysis (mean ± SD) are shown. *$p < 0.05$ and **$p < 0.01$ relative to control sample.

upregulated in the sample treated with the racemic mixture and in the one treated with (+)-MRJF4 enantiomer, while no significant change is observed in the other experimental points (Figure 7C).

Discussion

Prostate cancer is one of the most common cause of death in men. It is reported that pharmacological treatments, such as oridonin and atorvastatin, can inhibit the proliferation of prostatic cancer cells by inducing cell cycle arrest, apoptosis, and autophagy in PC3 cells (15, 16). Normally, in tumour cells the histone deacetylase is hyperactive and, thus, linked to an uncontrolled growth of cancer cells. This suggests that the inhibition of such enzyme, determining the acetylation of the histone, could be a suitable therapeutical target.

Histone deacetylase inhibitors usually induce growth arrest, differentiation, and cell death. While it is well known that HDACi mediate their biological effects through regulation of gene expression, DNA replication and repairment via direct histone hyperacetylation (10), recent reports have established a link between HDACi and ERS (11). Histone deacetylases act by recruiting misfolded proteins for transport to aggresome which switches on a cytoprotective response preventing proteotoxicity by compacting proteins and providing autophagic clearance (26, 27). Inhibition of this process seems to increase the cellular load of unwanted proteins which, by inducing ERS, switches on cell death through apoptosis, autophagy, or necrosis, thus suggesting that HDACi could be favourable therapeutic agents (28).

In the present paper, we report the effects of the racemic mixture and of the two separate enantiomers of a novel inhibitor, MRJF4, on the morphological and molecular mechanisms driving autophagic occurrence in PC3 prostatic cells. Here, in fact, the antiproliferative effect of 5 μM MRJF4 in PC3 was observed; conversely, when an annexin assay was performed, no difference

was evidenced in terms of apoptosis in the different experimental conditions. Thus, an autophagy cell death was hypothesized and investigated: even if an increased expression of LC3 autophagy marker was observed for both the enantiomers at early time points, the effect of (+)-MRJF4 is more pronounced and lasting. Moreover, the early inhibition of histone deacetylase seems to be properly correlated with the expression of the autophagy marker only for the R-(+)-configuration.

Protein degradation by basal constitutive autophagy is important to avoid accumulation of poly-ubiquitinated protein aggregates and to prevent development of diseases such as Huntington's, Parkinson's, and Alzheimer's, as well as cancer (29, 30).

The morphological modifications, observed mainly in the cells treated with the two enantiomers, indicate the presence of autophagosome-like structures and seem to correlate with LC3 expression.

Such modifications seem to be driven by a downregulation of pERK/NF-kB signaling pathway and a parallel up-regulation of *p21*, as already reported for other experimental models (13, 15, 31). In addition, being migration activity of tumour cells a marker of invasiveness and malignancy, the effect of our novel HDACi was also tested on cell migration and expression of MMP9, a protein reported as playing a crucial role in tumour angiogenesis, invasion and metastasis occurrence (19). Both the R-(+) and S-(-)-configurations show a decreased migration ability while the MMP-9 expression appears to be slightly increased by the (+)-MRJF4. Such controversial findings could be explained by the fact that even though metalloproteinases are commonly thought to be involved in cancer progression, they can also exert numerous other effects (Sorsa 2006).

So we can hypothesize that the R-(+)-enantiomer shows an early induction of histone 4 hyperacetylation, LC3 expression, and regulation of the pERK/NF-kB/p21 signaling pathway, followed by morphological modifications and growth inhibition at 24 h. On the other hand the timeline for the S-(-)-entantiomer is not clear, since the acetylaton induction occurs later than the LC3 expression. Such differences could be explained by the fact that our compounds are not only HDACi but also sigma-1 antagonists and sigma-2 agonists. The interaction of both MRJF4 enantiomers with the catalytic site of the 3D model HDAC4 has not been tested with a docking procedure. However, our results suggested that for the inhibition of HDAC4, the R-(+)-configuration showed a greater inhibition than the corresponding S-(-)-enantiomer, probably due to a more stable interaction, demonstrating a stereospecific and selective interaction of (+)-MRJF4 with the active site of HDAC4. We can also assume that (+)-MRJF4 after 15 h and 24 h loses its inhibitory capacity probably due to hydrolysis processes involving the ester bond between haloperidol metabolite II and phenylbutirric acid.

Thus, taken together our results showed that, starting from the evidence that histone modification plays an important role in the pathogenesis of various cancers and that in our experimental model (PC3 prostatic cancer cell line) the inhibition of histone 4 deacetylase enzyme results in anticancer activity, the novel MRJF4, with a major extent for the R-(+)-configuration, exerts anticancer activity through activation of the autophagic

pathway.

References

1. Gozuacik, D., Kimchi A., Autophagy as a cell death and tumor suppressor mechanism. *Oncogene* 2004, **23**: 2891-2906, DOI:10.1038/sj.onc.1207521.

2. Barth, S., Glick, D., MacLeod, K. F., Autophagy: assays and artifacts. *J. Pathol.* 2010, **221**: 117-124, doi:10.1002/path.2694.

3. Tanida, I., Ueno, T., Kominami, E., LC3 conjugation system in mammalian autophagy. *Int. J. Biochem. Cell. Biol.* 2004, **36**: 2503-2518, doi:10.1016/j.biocel.2004.05.009.

4. Ogier-Denis, E., Codogno, P., Autophagy: a barrier or an adaptive response to cancer. *Biochim. Biophys. Acta* 2003, **1603**: 113-128, doi:10.1016/S0304-419X(03)00004-0.

5. Bursch, W., Ellinger, A., Kienzl, H., Torok, L., Pandey, S., Sikorska, M., Walker, R., Hermann, R. S., Active cell death induced by the anti-estrogens tamoxifen and ICI 164384 in human mammary carcinoma cells (MCF-7) in culture: the role of autophagy. *Carcinogenesis* 1996, **17**: 1595-1607, doi: 10.1093/carcin/17.8.1595.

6. Kanzawa, T., Bedwell, J., Kondo, Y., Kondo, S., Germano, I. M., Inhibition of DNA repair for sensitizing resistant glioma cells to temozolomide. *J. Neurosurg.* 2003, **99**: 1047-1052, doi:10.3171/jns.2003.99.6.1047.

7. Drummond, D. C., Noble, C. O., Kirpotin, D. B., Guo, Z., Scott, G. K., Benz, C. C., Clinical development of histone deacetylase inhibitors as anticancer agents. *Annu. Rev. Pharmacol. Toxicol.* 2005, **45**: 495-528, doi: 10.1146/annurev.pharmtox.45.120403.095825.

8. Cacciatore, I., Caccuri, A.M., Cocco, A., De Maria, F., Di Stefano, A., Luisi, G., Pinnen, F., Ricci, G., Sozio, P., Turella, P., Potent isozyme-selective inhibition of human glutathione S-transferase A1-1 by a novel glutathione S-conjugate. *Amino Acids* 2005, **29**: 255-261, doi: 10.1007/s00726-005-0232-7.

9. Schontal, A. H., Endoplasmic reticulum stress and autophagy as targets for cancer therapy. *Cancer Lett.* 2009, **275**: 163-169, doi: 10.1016/j.canlet.2008.07.005.

10. Bolden, J., Peart, M. J., Johnstone, R. W. Anticancer activities of histone deacetylase inhibitors. *Nat. Rev. Drug. Discov.* 2006, **5**: 769-784, doi:10.1038/nrd2133.

11. Rodriguez-Gonzalez, A., Lin, T., Ikeda, A. K., Simms Waldrip, T., Fu, C., Sakamoto, K. M., Role of aggresome pathway in cancer: targeting histone deacetylase 6-dependent protein degradation. *Cancer Res.* 2008, **68**: 2557-2560, doi: 10.1158/0008-5472.CAN-07-5989.

12. Marrazzo, A., Fiorito, J., Zappalà, L., Prezzavento, O., Ronsisvalle, S., Pasquinucci, L., Scoto, G. M., Bernardini, R., Ronsisvalle, G., Antiproliferative activity of phenylbutyrate ester of haloperidol metabolite II [(±)-MRJF4] in prostate cancer cells. *Eur. J. Med. Chem.* 2011, **46**: 433-438, doi: 10.1016/j.ejmech.2010.10.012.

13. Pacella, S., Sozio, P., Di Giacomo, V., Patruno, A., Rapino, M., Marrazzo, A., Fiorito, J., Di Stefano, A., Cacciatore, I., Cataldi, A., Effect of histone deacetylase inhibitor MRJF4 on NF-kB and MMP9 molecular determinants of C6 glioma cells proliferation and migration. CNS Agents Med. Chem.2015, submitted.

14. Sozio, P., Fiorito, J., Di Giacomo, V., Di Stefano, A., Marinelli, L., Cacciatore, I., Cataldi, A., Pacella, S., Turkez, H., Parenti, C., Rescifina, A., Marrazzo, A., Haloperidol metabolite II prodrug: Asymmetric synthesis and biological evaluation on rat C6 glioma cells. *Eur. J. Med. Chem.* 2015, **90**: 1-9, doi: 10.1016/j.ejmech.2014.11.012.

15. Li, X., Li, X., Wang, J., Ye, Z., Li, J. C., Oridonin up-regulates expressionof *p21* and induces autophagy and apoptosis in human prostate cancer cells. *Int. J. Biol. Sci.* 2012, **8**: 901-912, doi:10.7150/ijbs.4554.

16. Peng, X., Li, W., Yuan, L., Mehta, R. J., Kopelovich, L., Mc Cormick, D. L., Inhibition of proliferation and induction of autophagy by atorvastatin in PC3 prostate cancer cells correlate with downregulation of Bcl2 and up-regulation of miR-182 and *p21*. *PLoS ONE* 2013, **8**: 70442, doi: 10.1371/journal.pone.0070442.

17. Chang, C. P., Su, Y. C., Lee, P. H., Lei, H. Y., Targeting NFKB by autophagy to polarize hepatoma-associated macrophage differentiation. *Autophagy* 2013, **9**: 619-621, doi: 10.4161/auto.23546.

18. Bjorklund, M., Koivunen, E., Gelatinase-mediated migration and invasion of cancer cells. *Biochim. Biophys. Acta* 2005, **1755**: 37-69, doi:10.1016/j.bbcan.2005.03.001.

19. Kessenbrock, K., Plaks, V., Werb, Z., Matrix metalloproteinases regulators of microenvironment. *Cell* 2010, **141**: 52-67, doi: 10.1016/j.cell.2010.03.015.

20. Kim, J., Lee, J. W., Kim, S. I., Choi, Y. J., Lee, W. K., Jeong, M. J., Cha, S. H., Lee, H. J., Chun, W., Kim, S. S., Thrombin induced migration of MMP9 expression are regulated by MAPK and PI3K pathways in C6 glioma cells. *Korean Physiol. Pharmacol*. 2011, **15**: 211-216, doi: 10.4196/kjpp.2011.15.4.211.

21. Cacciatore, I., Cornacchia, C., Fornasari, E., Baldassarre, L., Pinnen, F., Sozio, P., Di Stefano, A., Marinelli, L., Dean, A., Fulle, S., Di Filippo, E. S., La Rovere, R. M. L., Patruno, A., Ferrone, A., Di Marco, V., A glutathione derivative with chelating and in vitro neuroprotective activities: Synthesis, physicochemical properties, and biological evaluation. *Chem. Med. Chem*. 2013, **8**: 1818-1829, doi: 10.1002/cmdc.201300295.

22. Ronzoni, S., Faretta, M., Ballarini, M., Pelicci, P., Minucci, S., New method to detect histone acetylation levels by flow cytometry. *Cytometry A*. 2005, **66**: 52-61, doi: 10.1002/cyto.a.20151.

23. Patruno, A., Fornasari, E., Di Stefano, A., Cerasa, L. S., Marinelli, L., Baldassarre, L., Sozio, P., Turkez, H., Franceschelli, S., Ferrone, A., Di Giacomo, V., Speranza, L., Felaco, M., Cacciatore, I., Synthesis of a novel cyclic prodrug of S-allyl-glutathione able to attenuate LPS-induced ROS production through the inhibition of MAPK pathways in U937 cells. *Mol. Pharm*. 2015, **12**: 66-74, doi: 10.1021/mp500431r.

24. Pinnen, F., Sozio, P., Cacciatore, I., Cornacchia, C., Mollica, A., Iannitelli, A., D'Aurizio, E., Cataldi, A., Zara, S., Nasuti, C., Di Stefano, A. Ibuprofen and glutathione conjugate as a potential therapeutic agent for treating Alzheimer's disease. *Arch. Pharm*. 2011, **344**: 139-148, doi: 10.1002/ardp.201000209.

25. Euking, S., Iannitelli, A., Di Stefano, A., Borchard, G., Toll-like receptor-2 agonist functionalized biopolymer for mucosal vaccination. *Int. J. Pharm*. 2009, **381**: 97-105, doi: 10.1016/j.ijpharm.2009.03.039.

26. Kawaguchi, Y., Kovacs, J. J., McLaurin, A., Vance, J. M., Ito, A., Yao, T. P., The deacetylase HDAC6 regulates aggresome formation and cell viability in response to misfolded protein stress. *Cell* 2003, **115**: 727-738, doi:10.1016/S0092-8674(03)00939-5.

27. Pandey, U. B., Nie, Z., Batlevi, Y., Mc Gray, B. A., Ritson, G. P., Nedelsky, N. B., Schwartz, S. L., Di Prospero, N. A., Knight, M. A., Schuldiner, O., Padmanabhan, R., Hild, M., Berry, D. L., Garza, D., Hubbert, C. C., Yao, T. P., Baehrecke, E. H., Taylor, J. P., HDAC6 rescues neurodegeneration and provides an essential link between autophagy and the UPS. *Nature* 2007, **447**: 859-863, doi:10.1038/nature05853.

28. Minucci, S., Pelicci, P. G., Histone deacetylase inhibitors and the promise of epigenetic (and more) treatments for cancer. *Nature* 2006, **6**: 38-51, doi:10.1038/nrc1779.

29. Ma, Y., Hendershot, L. M., The role of the unfolded protein re-

sponse in tumourdevelopment: friend or foe? *Nat. Rev. Cancer* 2004, **4**: 966-977, doi:10.1038/nrc1505.

30. Eskelinen, E. L., Galfi, O., Autophagy: a lysosomal degradation pathway with central role in health and disease. *Biochim. Biophys. Acta* 2009, **1793**: 664-673, doi:10.1016/j.bbamcr.2008.07.014.

31. Pattingre, S., Bauvy, C., Codogno, P., Amino acids interfere with the ERK1/2 dependent control of macro autophagy by controlling the activation of Raf-1 in human colon cancer cells. *J. Biol. Chem.* 2003, **278**: 16667-16674, doi: 10.1074/jbc.M210998200.

32. Sorsa, T., Tjädherane, L., Konttine Y. T., Lauhio, A., Salo, T., Lee, H. M., Golub, L. M., Brown, D. L., Mäntylä, P., Matrix metalloproteinases: contribution to pathogenesis, diagnosis and treatment of periodontal inflammation. *Ann. Med.* 2006, **38**: 306-321, doi:10.1080/07853890600800103.